Applied Clay Science 153 (2018) 90–94

Contents lists available at ScienceDirect

Applied Clay Science

journal homepage: www.elsevier.com/locate/clay

Research paper

Effect of raw material milling on ceramic proppants properties

Anabella Mocciaro[a,*], Maria B. Lombardi[a,b], Alberto N. Scian[a,b]

[a] CETMIC Centro de Tecnología de Recursos Minerales y Cerámica (CIC-CONICET La Plata), Cno. Centenario y 506, M.B. Gonnet 1897, Argentina
[b] Departamento de Química Facultad de Ciencias Exactas, Universidad Nacional de La Plata, Calle 1 y 47, La Plata 1900, Argentina

ARTICLE INFO

Keywords:
Ceramic proppants
Milling
Low density
High breakage resistance
Kaolin
Bauxite

ABSTRACT

Low density and high breakage resistance ceramic proppants were developed from kaolin, bauxite and monoaluminum phosphate (MAP). The effect of the particle size on the raw materials over the density, the open porosity and the breakage resistance of the proppants was evaluated. The phase composition and the structure of the proppants due to the milling process were analyzed by X-ray diffraction (XRD), scanning electron microscopy (SEM) and pore size distribution by mercury intrusion. The proppants obtained with raw materials of smaller size improved its breakage resistance and developed a smaller open pore size, achieving an apparent density of 2.4 g/cm3 with a breakage ratio of 9.61% under 64 MPa. Some properties of the AG3 proppants with sand, low density ceramic proppants of the literature and commercial low density ceramics proppants were compared.

1. Introduction

Proppants are agents used in the hydraulic fracture process for the extraction of non-conventional gas and oil. This process involves the injection of a fracture liquid with solid spherical proppants at high pressure to break the rock and release the hydrocarbons. The purpose of the proppants is to help in the fracture, keeping the fracture walls open resisting the forces that tend to close it. Thus, proppants prevent the collapse of the fracture, forming the channels that increase the gas and oil conductivity (Kulkarni and Ochoa, 2012; Snegirev and Slobodin, 1998). There are different types of proppants: polymeric, quartz sands and ceramic materials (Liang et al., 2016; Yin and Dai, 2005; Zhao et al., 2015). The advantage of the first one is its low density; however, they do not have a great breakage resistance such as ceramic materials.

A low bulk density of the proppants allows them to be dragged by the fracture liquid with efficiency and prevent their accumulation in the first part of the fracture, which negatively influence in the whole conductivity. This indicates a need to develop a low density ceramic proppants with and acceptable breakage resistance (Bestaoui-Spurr and Hudson, 2017; Cutler et al., 1985; Gaurav et al., 2012; Gu et al., 2015).

Low density ceramic proppants are those with similar apparent density values as sand (2.60–2.65 g/cm^3) (Cannan and Palamara, 2006; Lunghofer, 1992).

Mullite ($3Al_2O_3{\cdot}2SiO_2$) is one of the main components of the ceramic proppants available in the market, due to its properties such as high mechanical strength, low thermal expansion coefficient and high resistance to acid corrosion (Aksay et al., 1991; Schneider et al., 2008).

These properties makes the mullite a suitable material for preparing proppants because of the closure stress and corrosive conditions that are subjected in the hydraulic fracture.

One of the synthesis methods to obtained mullite is by sintering kaolin with an alumina source (Al_2O_3), the solid phase reaction is: $3Al_2O_3 + 2SiO_2 \rightarrow 3Al_2O_3{\cdot}2SiO_2$ (Brindley and Nakahira, 1959; Burst, 1991; Chen et al., 2000).

Some researchers reported the milling of the raw materials but the final size of the particles is not specified (Liu et al., 2016; Wu et al., 2017; Zhao et al., 2015). Also some patents recommended an average particle size less than about 15 μm, preferably less than about 10 μm and most preferably, less than about 5 μm (Fitzgibbon and Lafayettw, 1984; Khaund, 1987).

In this work, mullite ceramic proppants were developed, studying how the particle size of the raw materials affects the bulk density, the breakage resistance and the structural properties. Also the low density ceramic proppants obtained were compared with sand, low ceramic proppants of the literature, and a commercial low ceramic proppant.

2. Materials and methods

2.1. Raw materials

A kaolin Tincar Super (Santa Cruz, Argentina) and bauxite (Brasil) were used as solid raw materials (Burst, 1991). Monoaluminum phosphate (MAP or $Al(H_2PO_4)_3$) solution was used as a phosphoric binder when it is exposed at temperature (Giskow et al., 2004; Kingery, 1950; Morris et al., 1977).

In this work, MAP was synthesized in the laboratory from a

* Corresponding author.
E-mail address: anamocciaro@cetmic.unlp.edu.ar (A. Mocciaro).

https://doi.org/10.1016/j.clay.2017.12.009
Received 19 May 2017; Received in revised form 8 December 2017; Accepted 9 December 2017
Available online 14 December 2017
0169-1317/

stoichiometric mixture of pseudobohemite ($Al_2O_3 \cdot xH_2O$) and phosphoric acid (H_3PO_4). The MAP obtained from the reaction was brought to a mass concentration of 40% and heated at 80 °C for 40 min to obtain a sol-gel system as the commercial solutions (Giskow et al., 2004).

The kaolin and bauxite powders were subjected to X-ray diffraction (XRD) analysis to determine their mineralogical composition using Cu kα radiation and a Ni filter at constant voltage 40 kV, and 35 mA using Philips PW-3710 Diffractometer.

Chemical analyses for the major oxides (mass %) of the kaolin and bauxite were performed using X-ray fluorescence spectrometry (XRF). Thermo gravimetric analysis (TG) and differential thermal analysis (DTA) of the raw materials was done up to 1300 °C by Rigaku Evo plus II TG-DTA Instrument. Both thermal analyses were carried out simultaneously at a 10 °C/min heating rate in air atmosphere (TG-DTA Rigaku Evo plus II, Japan).

The percentage of both bauxite and MAP used was 10%, based on the mass of clay. The roll of bauxite is to increase the amount of mullite in the proppants after thermal treatment.

2.2. Experimental procedures

Initially the solids were wet milled in porcelain ball mill for 48 h, 72 h, and 48 h with the addition of a dispersant (sodium polyacrylate). These mixtures were referred as AG1, AG2 and AG3 respectively. The particle size distribution obtained in each milling was determined using a laser diffraction based size analyzer using a Mastersizer 2000 Malvern Instrument.

The dispersions obtained by milling were dried at 110 °C and the agglomerates were broken using a hammer mill with a powder outlet of < 70 μm.

With a high energy mixer (R20E, Erich Industrial Ltd., Brazil), the green bodies proppants were formed from the mixtures of solids with the three milling parameters mentioned above (48 h, 72 h and 48 h with the addition of dispersant) and with the addition of MAP and water. The spherical green proppants were calcined in an electric furnace at air atmosphere with a heating rate of 5 °C/min until 1450 °C with a residence time of 1 h.

After calcination, the proppants were sieved through the 20/50 meshes (one of the sizes required for hydraulic fracture), and bulk density, apparent density, sphericity, roundness and breakage ratio at 64 MPa, were tested by API 19C standards (API 19C, 2008). Complementary tests, pore size distribution, X-ray diffraction and scanning electron microscopy analysis, were performed in order to understand the results.

2.2.1. Bulk and apparent density test

Bulk density, describes the mass of proppants that fills a unit volume and includes both the proppants and the spaces generated between them. In contrast, the apparent density is measured by picnometry and the mass of the material is evaluated per unit of volume of the proppants including the internal porosity.

2.2.2. Sphericity and roundness test

Sphericity is a measure of how much the proppants approaches to the sphere shape, and the roundness is a relative measure of the curvature and not the sharpness of the edges of the proppants. The standard API 19C says that ceramic proppants must have an average sphericity and an average roundness equal to or > 0.7.

2.2.3. Breakage ratio test

The breakage ratio is a measure of the mechanical strength of the proppants, and the equipment used is strictly following the API 19C standards. It is to determine the amount of proppants crushed at a given stress, the breakage ratio is calculated by the formula: $\eta = Wc / Wo \times 100\%$, where Wc is the weight of crushed specimens after testing and Wo is the weight of proppants before testing. The standard API 19C requires a $\eta \leq 10\%$ to be used for the hydraulic fracture.

Table 1
Chemical composition of kaolin and bauxite.

	Kaolin (%mass)	Bauxite (%mass)
SiO_2	61.82	13.38
Al_2O_3	27.55	53.91
Fe_2O_3	0.79	6.2
MgO	0.66	0.48
K_2O	0.76	0.22
TiO_2	0.39	0.72
Others	3.20	0.77
LOI (1000 °C)	7.63	24.33

2.2.4. Porosimetry test

The pore size distribution was analyzed by mercury intrusion porosimetry (Pascal-Thermo Fisher 440 and 140). It allows to know the *meso* and macro open porosity in the proppants as a relationship with the final density. Pores in the material can be determined by the volume of mercury, which is a non-wetting liquid.

2.2.5. X-ray diffraction (XRD) and scanning electron microscopy (SEM)

The crystalline phases and the structural changes due to the milling process present in the proppants were identified by X-ray diffraction. The morphology and microstructural characterization of the proppants were carried out by scanning electron microscopy (JEOL CM-600 Neo Scope). In order to reveal mullite grains, chemical etching was done with 5% hydrofluoric acid (HF) for 5 min (Elssner et al., 1999).

3. Results and discussion

The chemical composition of the raw materials was determined and showed the composition (mass %) of the samples in Table 1. The main components of the clay as oxides were alumina (Al_2O_3) and silica (Si_2O). The main components of the bauxite as oxides were Al_2O_3, Si_2O, Fe_2O_3 and Ti_2O indicating that was a low-grade bauxite (Liu et al., 2016; Ma et al., 2016).

The X-ray diffraction spectra of the kaolin (Fig. 1a) and the bauxite (Fig. 1b) showed the predominant crystalline phases. The kaolin sample revealed the presence of kaolinite and quartz (Moore and Reynolds, 1997; Zbik et al., 2010). In the bauxite sample X-ray diffraction spectra reflections associated with gibbsite ($Al(OH)_3$) and boehmite (AlO(OH)) were identified as the main sources of alumina; also, kaolinite, anatase (Ti_2O) and goethite (FeO(OH)) were observed.

The DTA curve of kaolin (Fig. 2a) showed two endothermic peaks at 74.8 °C and 512.8 °C and an exothermic peak at 983.9 °C. The first endothermic peak was relative to the dehydration of the clay and correlating with this in the TG curve at 21–200 °C there was a mass loss of 2%. The second endothermic peak on the DTA curve and a mass loss of 7% on the TG curve in the range of 200–800 °C was induced by the dehydroxylation of kaolinite. The exothermic peak, at 938.9 °C corresponded to the metakaolin-mullite transformation (Lee et al., 1999; Saikia et al., 2003).

Two endothermic peaks were observed on the bauxite DTA curve (Fig. 2b). The first peak at 298.9 °C was induced by the dehydration of $Al(OH)_3$ into AlO(OH) and corresponding to this peak a mass loss (− 22%) was observed from 200 to 380 °C in the TG curve. The second peak at 480 °C was induced by the dehydration of AlO(OH) into amorphous Al_2O_3 and related with this dehydration a mass loss (− 5%) was observed in the TG curve at the range of 400–650 °C (Laskou et al., 2006; Zhu et al., 2010).

The particle size distribution of the mixes with different millings process was determined (Fig. 3) and the maximum diameters in μm of 10%, 50% and 90% ($d_{0.1}$, $d_{0.5}$ and $d_{0.9}$ respectively) of each sample

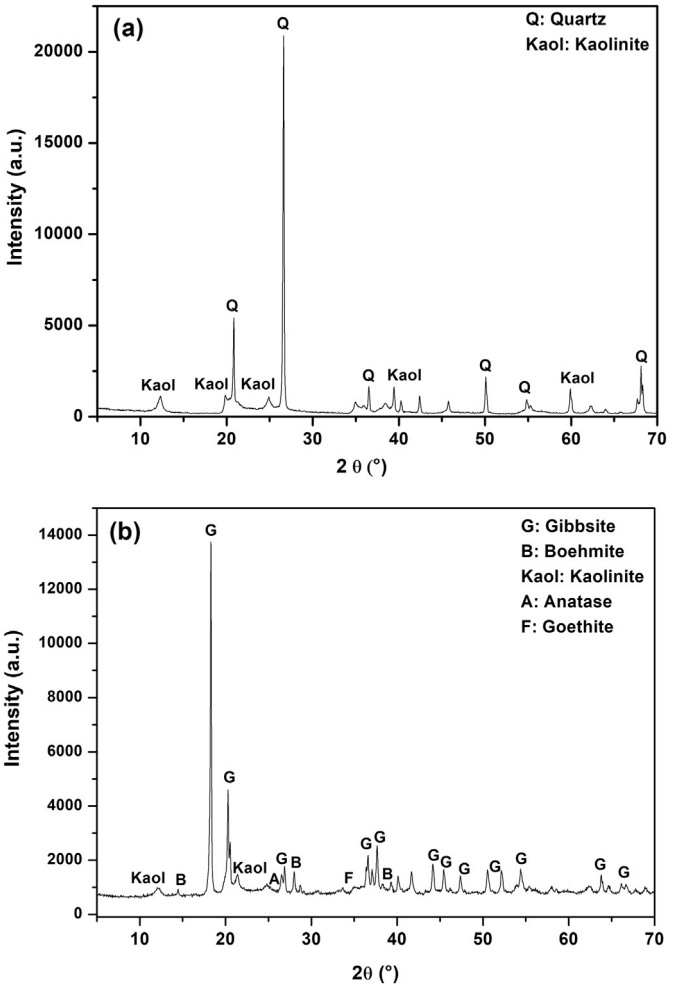

Fig. 1. X-ray diffraction spectra (Cu Kα) of kaolin (a) and bauxite (b).

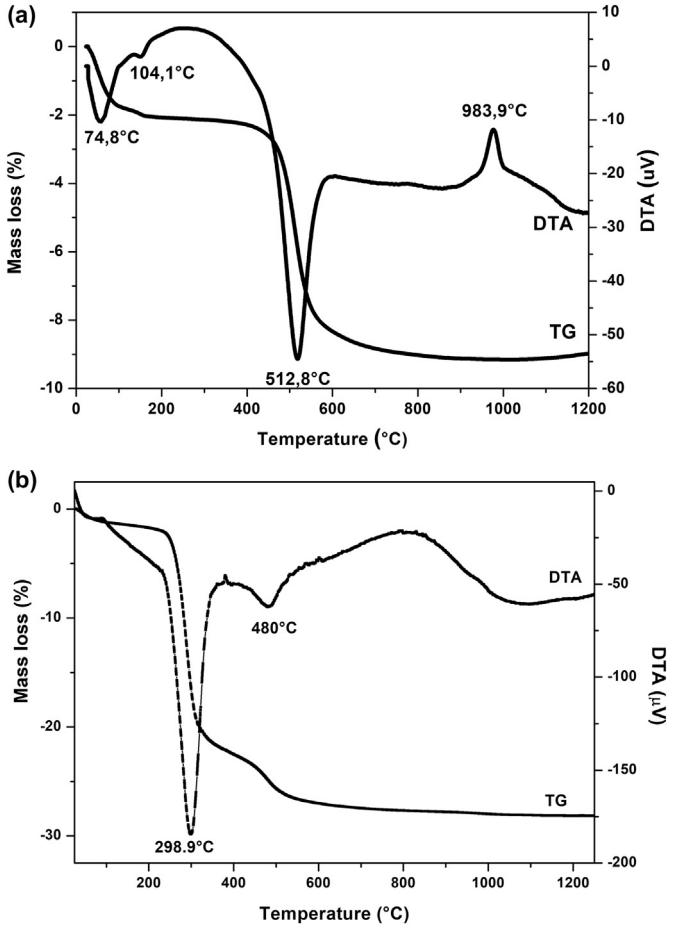

Fig. 2. DTA and TG curves of kaolin (a) and bauxite (b).

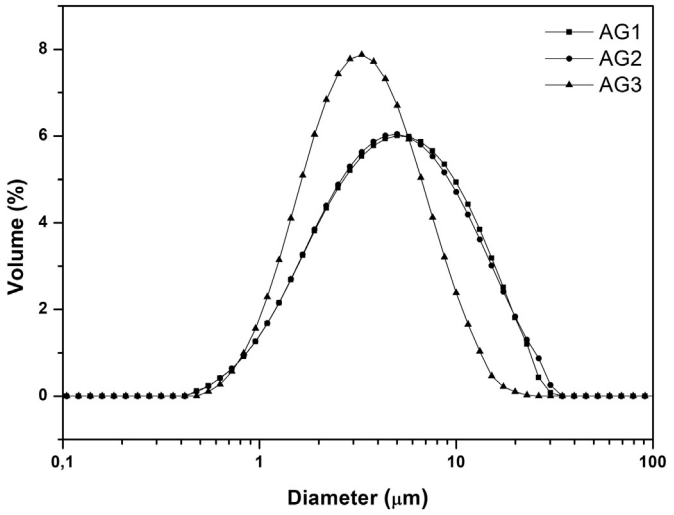

Fig. 3. Distribution of particle size.

presented in Table 2. No significant changes were found between AG1 and AG2 regarding the particle size distribution, however, in AG3 the distribution narrows with a smaller particle size and a large decreased in $d_{0.9}$. These milling results confirmed that the particle size obtained is notable influenced by the dispersant addition than by the time. This could be because the dispersant collaborates with the homogenous distribution of the material and prevents its agglomeration.

The size distribution of open pores by the mercury intrusion technique was determined for proppants. The open porosity distributions of macropores and mesopores (Fig. 4a and b respectively) revealed that the milling influences the open porosity of the material obtained and that the lower values of total pore volume were obtained for AG3.

As it is known, for low density ceramic proppants is required a low open porosity and also a significant closed porosity in order to obtain high strength resistance material.

The results of the characterization tests of proppants performed under API 19C standards were displayed in Table 3. The breakage ratio was evaluated under 64 MPa and the percentage of fine materials obtained due to the breakage ratio test varied with raw materials particle size. The lower breakage ratio was obtained when the smallest particle size was used, corresponding also with the lowest open porosity of the material (AG3).

The strength resistance of ceramics materials was mostly related to the size and amount of macropores than to the size and amount of mesopores.

The sphericity, roundness and the bulk density of the proppants were independent of the particle size of the raw materials used (Table 3).

Table 2
Maximum diameter in μm of 10%, 50% and 90% of the particles.

	AG1 [μm]	AG2 [μm]	AG3 [μm]
d (0.1)	1.440	1.438	1309
d (0.5)	4.495	4.436	3082
d (0.9)	12.789	13.013	7.337

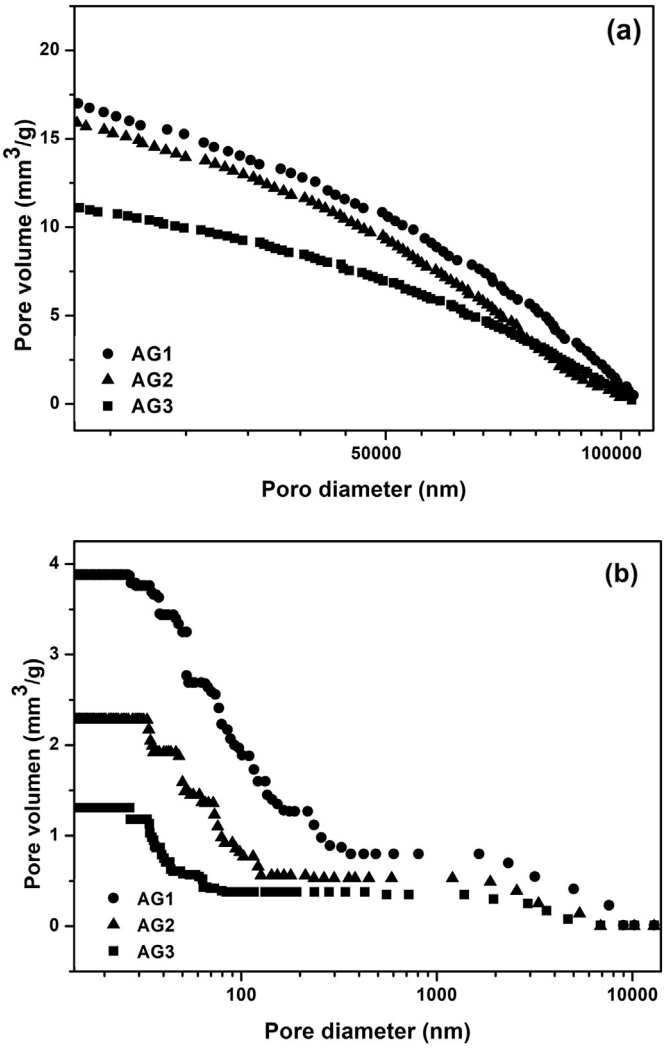

Fig. 4. Distribution of the macropore (a) and mesopore (b) pore size of the proppants AG1, AG2 and AG3.

Table 3
Proppants characterization, API 19C standards.

Sample	Bulk density (g/cm^3)	Apparent density (g/cm^3)	Sphericity-roundness	Breakage ratio (64 MPa)
AG1	1.33	2.32	0.8–0.6	12,36%
AG2	1.34	2.35	0.8–0.6	10.73%
AG3	1.33	2.40	0.8–0.6	9.61%

The apparent density of the materials increased as the particle size and the open porosity of the proppants decreased. AG3 proppants had the best performance with the lowest breakage ratio (9.61% under 64 MPa) and kept a low material density (2.4 g/cm^3).

Some properties of the AG3 proppants with sand, low ceramic proppants (Wu et al., 2017), and low ceramic proppant from Carbo Company were compared in Table 4. The AG3 proppants had the best performance, the lowest density and breakage ratio, comparing with others proppants (Table 4.)

The X-ray diffraction spectra of the proppants (Fig. 5) showed the crystalline phases mullite ($3Al_2O_3{\cdot}2SiO_2$) and cristobalite (SiO_2) with some percentage of amorphous phase. At 1450 °C the contribution of mullite coming from the thermal transformation of kaolinite and the secondary mullite produced by reaction between the reaming silica from kaolin and the alumina from bauxite (Chen et al., 2000; Liu et al., 1994). The analyses of the diffractograms confirmed that there were no variation between the crystalline phases for the different materials.

Table 4
Comparison of performance of AG3 proppants with sand, low ceramic proppants (Wu et al., 2017) and low ceramic Carbo Company proppants.

Sample	Phase composition	Bulk density (g/cm^3)	Apparent density (g/cm^3)	Breakage ratio
Sand	Quartz	1.50	2.64	9.0% (48 MPa)
Proppants (Wu et al., 2017)	Mullite	–	2.61	5.0% (52 MPa)
Carbo econoprop	Mullite Cristobalite	1.56	2.7	2.8% (52 MPa)
AG3	Mullite Cristobalite	1.33	2.4	9.61% (64 MPa)

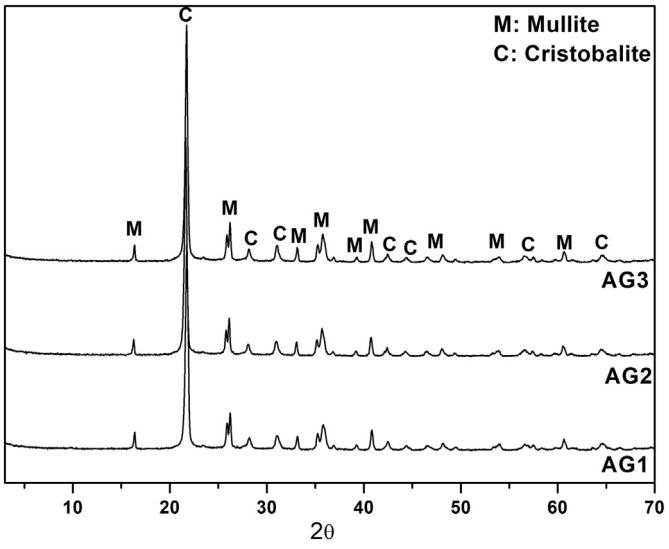

Fig. 5. X-ray diffraction spectra (Cu Kα) of the proppants AG1, AG2 and AG3.

The microstructure of materials AG1, AG2 and AG3 was analyzed by SEM micrograph (Fig. 6a, b and c respectively). In all materials acicular crystalline grains, characteristic of mullite (Santana et al., 2017), with some liquid phase generated at high temperature were observed. The microstructure of AG3 showed more macropores than the other materials (Fig. 6c), so it confirmed that this macropores observed were closed pores because AG3 material had the lower open porosity (Fig. 4).

4. Conclusions

The results of the study allowed to conclude that:

The milling of the raw materials (kaolin and bauxite) influences some properties of the obtained proppants.

The smallest particle size and the narrowest distribution were obtained when the solid raw materials were milled for 48 h with the addition of a dispersant.

The apparent density of the ceramic proppants obtained with kaolin and both bauxite and MAP 10% was 2.32–2.40 g/cm^3. These values of density were lower than the sand and the others low density ceramic proppants compared in this work.

The particle size of the raw materials does not influence the proppants sphericity and roundness.

The smallest particle size of raw materials obtained, improve the performance at the breakage ratio at 64 MPa and decrease the open porosity of the ceramic proppants developed.

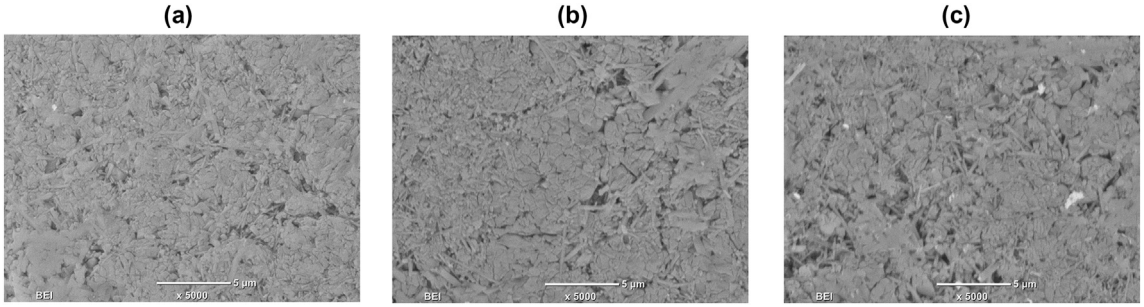

Fig. 6. SEM micrographs (5000 ×) of the proppants AG1 (a), AG2 (b) and AG3 (c).

Acknowledgements

This work has been partially supported by Nano-Petro FONARSEC Project 2012 (ANPCyT). AM acknowledges CONICET and Y-Tec for the fellowship.

References

Aksay, I.A., Dabbs, D.M., Sarikaya, M., 1991. Mullite for structural, electronic, and optical applications. J. Am. Ceram. Soc. 74, 2343–2358.
API 19C, 2008. Measurement of Properties of Proppants Used in Hydraulic Fracturing and Gravel-Packing Operations, 1st. ed. American Petroleum Institute.
Bestaoui-Spurr, N., Hudson, H., 2017. Ultra-Light weight proppant and pumping design lead to greater conductive fracture area in unconventional reservoirs. In: SPE Oil and Gas India Conference and Exhibition. Society of Petroleum Engineers, Mumbai India.
Brindley, G.W., Nakahira, M., 1959. The kaolinite_mullite reaction series: II, metakaolin. J. Am. Ceram. Soc. 42, 314–318.
Burst, J.F., 1991. The application of clay minerals in ceramics. Appl. Clay Sci. 5, 421–443.
Cannan, C.D., Palamara, T.C., 2006. Low density proppant. US7036591 B2.
Chen, C.Y., Lan, G.S., Tuan, W.H., 2000. Preparation of mullite by the reaction sintering of kaolinite and alumina. J. Eur. Ceram. Soc. 20, 2519–2525.
Cutler, R.A., Ennis, D.O., Jones, A.H., Swanson, S.R., 1985. Fracture conductivity comparison of ceramic proppants. Soc. Pet. Eng. J. 25, 157–170.
Elssner, G., Hoven, H., Kiessler, G., Wellner, P., 1999. Ceramics and ceramic composites: materialographic preparation, 1st. ed. Elsevier Science, New York, pp. 42.
Fitzgibbon, J.J., Lafayettw L., 1984. Sintered spherical pellets containing clay as mayor component useful for gas and oil well proppants. US 4427068.
Gaurav, A., Dao, E.K., Mohanty, K.K., 2012. Evaluation of ultra-light-weight proppants for shale fracturing. J. Pet. Sci. Eng. 92–93, 82–88.
Giskow, R., Lind, J., Schmidt, E., 2004. The variety of phosphates for refractory and technical applications by the example of aluminum phosphates. CFI Ceram. Forum Int. 81, E27–E32.
Gu, M., Dao, E., Mohanty, K.K., 2015. Investigation of ultra-light-weight proppant application in shale fracturing. Fuel 150, 191–201.
Khaund, A., 1987. Sintered low density gas and oil well proppants from a low cost unblended clay material of selected composition. US 4668645 A.
Kingery, W.D., 1950. Fundamental study of phosphate bonding in refractories: I, literature review. J. Am. Ceram. Soc. 33, 239–241.
Kulkarni, M.C., Ochoa, O.O., 2012. Mechanics of light weight proppants: a discrete approach. Compos. Sci. Technol. 72, 879–885.
Laskou, M., Margomenou-Lenidopoulou, G., Balek, V., 2006. Thermal characterization of bauxite samples. J. Therm. Anal. Calorim. 84, 141–146.
Lee, S., Kim, Y.J., Moon, H.S., 1999. Phase transformation sequence from kaolinite to mullite investigated by an energy-filtering transmission electron microscope. J. Am. Ceram. Soc. 82, 2841–2848.
Liang, F., Sayed, M., Al-Muntasheri, G.A., Chang, F.F., Li, L., 2016. A comprehensive review on proppant technologies. Petroleum 2, 26–39.
Liu, K.C., Thomas, G., Caballero, A., Moya, J.S., De Aza, S., 1994. Mullite formation in kaolinite-α-alumina. Acat Metall. Mater. 42, 489–495.
Liu, Z., Zhao, J., Li, Y., Zeng, Z., Mao, J., Peng, Y., He, Y., 2016. Low-temperature sintering of bauxite-based fracturing proppants containing CaO and MnO_2 additives. Mater. Lett. 171, 300–303.
Lunghofer, E.P., 1992. Hydraulic fracturing propping agent. US5120455 A.
Ma, X., Tian, Y., Zhou, Y., Wang, K., Chai, Y., Li, Z., 2016. Sintering temperature dependence of low-cost, low-density ceramic proppant with high breakage resistance. Mater. Lett. 180, 127–129.
Moore, D.M., Reynolds, R.C., 1997. X-Ray Diffraction and the Identification and Analysis of Clay Minerals, 2nd. ed. Oxford University Press, Oxford, New York.
Morris, J.H., Perkins, P.G., Rose, A.E.A., Smith, W.E., 1977. The chemistry and binding properties of aluminum phosphates. Chem. Soc. Rev. 6, 173–194.
Saikia, N.J., Bharali, D.J., Sengupta, P., Bordoloi, D., Goswamee, R.L., Saikia, P.C., Borthankur, P.C., 2003. Characterization, beneficiation and utilization of a kaolinite clay from Assam, India. Appl. Clay Sci. 24, 93–103.
Santana, L.N.L., Gomes, J., Menezes, R.R., Neves, G.A., Lira, H.L., Segadães, A.M., 2017. Microstructure development in clays upon heat treatment: kinetics and equilibrium. Appl. Clay Sci. 135, 325–332.
Schneider, H., Schreuer, J., Hildmann, B., 2008. Structure and properties of mullite- a review. J. Eur. Ceram. Soc. 28, 329–344.
Snegirev, A.I., Slobodin, B.V., 1998. Manufacturing process and properties of spherical granules in the MgO-Al_2O_3-SiO_2 system. Refract. Ind. Ceram. 39, 372–374.
Wu, X., Hou, Z., Ren, Q., Li, H., Lin, F., Wei, T., 2017. Preparation and characterization of ceramic proppants with low density and high strength using fly ash. J. Alloys Compd. 702, 442–448.
Yin, X., Dai, Y., 2005. Characteristics, manufacture and application of colloidal silica. Chem. Propellants Polym. Mater. 3, 27–31.
Zbik, M.S., Raftery, N.A., Smart, R.S.C., Frost, R.L., 2010. Kaolinite platelet orientation form XRD and AFM applications. Appl. Clay Sci. 50, 299–304.
Zhao, J., Liu, Z., Li, Y., 2015. Preparation and characterization of low-density mullite-based ceramic proppant by a dynamic sintering method. Mater. Lett. 152, 72–75.
Zhu, B., Fanf, B., Li, X., 2010. Dehydration reactions and kinetic parameters of gibbsite. Ceram. Int. 36, 2493.